DOI: 10.17277/amt.2016.01.pp.061-066

Sampling Surfaces Formulation for Functionally Graded and Laminated Composite Shells

G.M. Kulikov*, A.A. Mamontov, S.V. Plotnikova, M.G. Kulikov, S.A. Mamontov

Department of Applied Mathematics and Mechanics, Tambov State Technical University, 106, Sovetskaya, Tambov, 392000, Russian Federation

* Corresponding author. Tel.: + 7 (4752) 63 04 41. *E-mail: gmkulikov@mail.ru*

Abstract

This paper focuses on a finite element implementation of the sampling surfaces (**SaS**) method for the three-dimensional (**3D**) stress analysis of functionally graded (**FG**) laminated elastic and electroelastic shells. The SaS formulation is based on choosing inside the *n*th layer I_n not equally spaced SaS parallel to the middle surface of the shell in order to introduce the electric potentials and displacements of these surfaces as basic shell variables. Such choice of unknowns permits the presentation of the proposed FG shell formulation in a very compact form. The SaS are located inside each layer at Chebyshev polynomial nodes that improves the convergence of the SaS method significantly.

Keywords

Functionally graded material; laminated piezoelectric shell; sampling surfaces method, exact geometry solid-shell element.

Introduction

The exact 3D analysis of FG piezoelectric shells has received considerable attention during past ten years. There are at least five approaches to the exact 3D analysis of electroelasticity for FG piezoelectric laminated shells, namely, the modified Pagano approach, the series expansion approach, the state space approach, the asymptotic approach and the SaS approach. The first four approaches were applied efficiently to the 3D analysis of FG piezoelectric structures in many papers [1]. Recently, the SaS approach has been also applied to the 3D modelling of FG piezoelectric plates and shells [2–4].

In accordance with the SaS method, we choose inside the *n*th layer I_n not equally spaced SaS $\Omega^{(n)1}, \Omega^{(n)2},..., \Omega^{(n)I_n}$ parallel to the middle surface and introduce displacement vectors $\mathbf{u}^{(n)1}, \mathbf{u}^{(n)2},..., \mathbf{u}^{(n)I_n}$ and electric potentials $\varphi^{(n)1}, \varphi^{(n)2},..., \varphi^{(n)I_n}$ of these surfaces as basic shell variables, where $I_n \geq 3$. Such choice of displacements and electric potentials with the consequent use of Lagrange polynomials of degree $I_n - 1$ in the thickness direction for each layer permits the presentation of governing equations of the FG piezoelectric laminated shell formulation in a very compact form.

It is worth noting that the developed approach with equally spaced SaS does not work properly with Lagrange polynomials of high degree because of the Runge's phenomenon, which yields the wild oscillation at the edges of the interval when the user deals with any specific functions. If the number of equally spaced nodes is increased then the oscillations become even larger. However, the use of Chebyshev polynomial nodes allows one to minimize uniformly the error due to Lagrange interpolation. This fact gives an opportunity to find solutions of the 3D static problems of elasticity and electroelasticity for FG laminated shells with a prescribed accuracy employing the sufficiently large number of SaS.

SaS Formulation for Displacement and Strain Fields

Consider a thick laminated shell of the thickness h. Let the middle surface Ω be described by orthogonal curvilinear coordinates θ_1 and θ_2, which are referred to the lines of principal curvatures of its surface. The coordinate θ_3 is oriented along the unit vector $\mathbf{e}_3$ normal to the middle surface. Introduce the following notations: $\mathbf{e}_\alpha$ are the orthonormal base vectors of the middle surface; A_α are the coefficients of the first fundamental form; k_α are the principal curvatures of the middle surface; $c_\alpha^{(n)i_n} = 1 + k_\alpha \theta_3^{(n)i_n}$ are the components of the shifter tensor at SaS; $\theta_3^{(n)i_n}$ are the transverse coordinates of SaS inside the nth layer given by:

$$\theta_3^{(n)1} = \theta_3^{[n-1]}, \quad \theta_3^{(n)I_n} = \theta_3^{[n]}, \tag{1}$$

$$\theta_3^{(n)m_n} = \frac{1}{2}\left(\theta_3^{[n-1]} + \theta_3^{[n]}\right) - \frac{1}{2} h_n \cos\left(\pi \frac{2m_n - 3}{2(I_n - 2)}\right), \tag{2}$$

where $\theta_3^{[n-1]}$ and $\theta_3^{[n]}$ are the transverse coordinates of layer interfaces $\Omega^{[n-1]}$ and $\Omega^{[n]}$ depicted in Fig. 1; $h_n = \theta_3^{[n]} - \theta_3^{[n-1]}$ is the thickness of the nth layer. Here and in the following developments, the index n identifies the belonging of any quantity to the nth layer and runs from 1 to N, where N is the number of layers; the index m_n identifies the belonging of any quantity to the inner SaS of the nth layer and runs from 2 to $I_n - 1$, whereas the indices i_n, j_n, k_n to be used later describe all SaS of the nth layer and run from 1 to I_n;

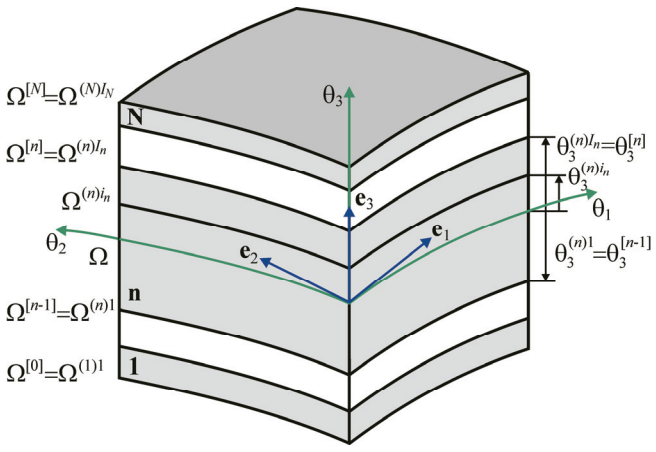

Fig. 1. Geometry of the laminated shell

Greek indices α, β range from 1 to 2; Latin tensorial indices i, j, k, l range from 1 to 3.

It is seen from (2) that transverse coordinates of inner SaS of the nth layer coincide with coordinates of the Chebyshev polynomial nodes [5]. This fact has a great meaning for a convergence of the SaS method [6].

The strain tensor at SaS of the nth layer in a middle surface frame $\mathbf{e}_i$ can be written as follows [6]:

$$2\varepsilon_{\alpha\beta}^{(n)i_n} = \frac{1}{c_\beta^{(n)i_n}} \lambda_{\alpha\beta}^{(n)i_n} + \frac{1}{c_\alpha^{(n)i_n}} \lambda_{\beta\alpha}^{(n)i_n},$$

$$2\varepsilon_{\alpha 3}^{(n)i_n} = \beta_\alpha^{(n)i_n} + \frac{1}{c_\alpha^{(n)i_n}} \lambda_{3\alpha}^{(n)i_n}, \quad \varepsilon_{33}^{(n)i_n} = \beta_3^{(n)i_n}, \tag{3}$$

where $\lambda_{i\alpha}^{(n)i_n}$ are the strain parameters of SaS defined as:

$$\lambda_{\alpha\alpha}^{(n)i_n} = \frac{1}{A_\alpha} u_{\alpha,\alpha}^{(n)i_n} + B_\alpha u_\beta^{(n)i_n} + k_\alpha u_3^{(n)i_n},$$

$$\lambda_{\beta\alpha}^{(n)i_n} = \frac{1}{A_\alpha} u_{\beta,\alpha}^{(n)i_n} - B_\alpha u_\alpha^{(n)i_n} \quad \text{for} \quad \beta \neq \alpha,$$

$$\lambda_{3\alpha}^{(n)i_n} = \frac{1}{A_\alpha} u_{3,\alpha}^{(n)i_n} - k_\alpha u_\alpha^{(n)i_n},$$

$$B_\alpha = \frac{1}{A_\alpha A_\beta} A_{\alpha,\beta} \quad \text{for} \quad \beta \neq \alpha, \tag{4}$$

where $u_i^{(n)i_n} = u_i(\theta_3^{(n)i_n})$ are the displacements of SaS; $\beta_i^{(n)i_n} = u_{i,3}(\theta_3^{(n)i_n})$ are the derivatives of displacements with respect to thickness coordinate at SaS.

Now, we start with the first assumption of the proposed piezoelectric laminated shell formulation. Let us assume that displacements of the nth layer $u_i^{(n)}$ are distributed through the thickness as follows:

$$u_i^{(n)} = \sum_{i_n} L^{(n)i_n} u_i^{(n)i_n}, \quad \theta_3^{[n-1]} \le \theta_3 \le \theta_3^{[n]}, \tag{5}$$

where $L^{(n)i_n}(\theta_3)$ are the Lagrange polynomials of degree $I_n - 1$ expressed as

$$L^{(n)i_n} = \prod_{j_n \neq i_n} \frac{\theta_3 - \theta_3^{(n)j_n}}{\theta_3^{(n)i_n} - \theta_3^{(n)j_n}}. \tag{6}$$

Using equations (5) and (6), one obtains

$$\beta_i^{(n)i_n} = \sum_{j_n} M^{(n)j_n}\left(\theta_3^{(n)i_n}\right) u_i^{(n)j_n}, \qquad (7)$$

where $M^{(n)j_n} = L_{,3}^{(n)j_n}$ are the derivatives of the Lagrange polynomials. It is seen that the key functions $\beta_i^{(n)i_n}$ of the laminated shell formulation are represented according to (7) as a *linear combination* of displacements of SaS of the *n*th layer $u_i^{(n)j_n}$.

The following step consists in a choice of the suitable approximation of strains through the thickness of the *n*th layer. It is apparent that the strain distribution should be chosen similar to the displacement distribution (5). Thus, the second assumption of the developed shell formulation can be written as

$$\varepsilon_{ij}^{(n)} = \sum_{i_n} L^{(n)i_n}\varepsilon_{ij}^{(n)i_n}, \quad \theta_3^{[n-1]} \le \theta_3 \le \theta_3^{[n]}. \qquad (8)$$

The strain-displacement relationships (3) and (8) exactly represent all rigid-body motions of the laminated shell in any convected curvilinear coordinate system. The proof of this statement is given in paper [6].

SaS Formulation for Electric Field

The relation between the electric field E_i and the electric potential φ is given by

$$E_\alpha = -\frac{1}{A_\alpha(1+k_\alpha\theta_3)}\varphi_{,\alpha}, \quad E_3 = -\varphi_{,3}. \qquad (9)$$

In particular, the electric field at SaS of the *n*th layer $E_i^{(n)i_n} = E_i\left(\theta_3^{(n)i_n}\right)$ is presented as

$$E_\alpha^{(n)i_n} = -\frac{1}{A_\alpha c_\alpha^{(n)i_n}}\varphi_{,\alpha}^{(n)i_n}, \quad E_3^{(n)i_n} = -\psi^{(n)i_n}, \qquad (10)$$

where $\varphi^{(n)i_n} = \varphi\left(\theta_3^{(n)i_n}\right)$ are the electric potentials of SaS of the *n*th layer; $\psi^{(n)i_n} = \varphi_{,3}(\theta_3^{(n)i_n})$ are the values of the derivative of the electric potential with respect to thickness coordinate on SaS.

Next, we accept the third and fourth assumptions of the proposed piezoelectric laminated shell formulation. Let the electric potential and the electric field be distributed through the thickness of the *n*th layer as follows [3]:

$$\varphi^{(n)} = \sum_{i_n} L^{(n)i_n}\varphi^{(n)i_n}, \ \theta_3^{[n-1]} \le \theta_3 \le \theta_3^{[n]}, \qquad (11)$$

$$E_i^{(n)} = \sum_{i_n} L^{(n)i_n} E_i^{(n)i_n}, \ \theta_3^{[n-1]} \le \theta_3 \le \theta_3^{[n]}. \qquad (12)$$

The use of (6) and (11) yields a simple formula

$$\psi^{(n)i_n} = \sum_{j_n} M^{(n)j_n}(\theta_3^{(n)i_n})\varphi^{(n)j_n}, \qquad (13)$$

which is similar to (7). This implies that the key functions $\psi^{(n)i_n}$ of the piezoelectric laminated shell formulation are represented as a *linear combination* of electric potentials of SaS of the *n*th layer $\varphi^{(n)j_n}$.

Variational Formulation

The variational equation for the piezoelectric laminated shell in the case of conservative loading can be written as

$$\delta\Pi = 0, \qquad (14)$$

where Π is the extended potential energy defined as

$$\Pi = \frac{1}{2}\iint_\Omega \sum_n \int_{\theta_3^{[n-1]}}^{\theta_3^{[n]}} \left(\sigma_{ij}^{(n)}\varepsilon_{ij}^{(n)} - D_i^{(n)}E_i^{(n)}\right) A_1A_2 \times$$

$$\times(1+k_1\theta_3)(1+k_2\theta_3)d\theta_1d\theta_2d\theta_3 - W, \qquad (15)$$

where $\sigma_{ij}^{(n)}$ is the stress tensor of the *n*th layer; $D_i^{(n)}$ is the electric displacement vector of the *n*th layer; W is the work done by external electromechanical loads.

Substituting strain and electric field distributions (8) and (12) in the extended potential energy (15) and introducing stress resultants and electric displacement resultants

$$H_{ij}^{(n)i_n} = \int_{\theta_3^{[n-1]}}^{\theta_3^{[n]}} \sigma_{ij}^{(n)} L^{(n)i_n}(1+k_1\theta_3)(1+k_2\theta_3)d\theta_3, \qquad (16)$$

$$T_i^{(n)i_n} = \int_{\theta_3^{[n-1]}}^{\theta_3^{[n]}} D_i^{(n)} L^{(n)i_n}(1+k_1\theta_3)(1+k_2\theta_3)d\theta_3, \qquad (17)$$

one finds

$$\Pi = \frac{1}{2}\iint_\Omega \sum_n \sum_{i_n}\left(H_{ij}^{(n)i_n}\varepsilon_{ij}^{(n)i_n} - T_i^{(n)i_n}E_i^{(n)i_n}\right)\times$$

$$\times A_1A_2d\theta_1d\theta_2 - W. \qquad (18)$$

For simplicity, we consider the case of linear piezoelectric materials

$$\sigma_{ij}^{(n)} = C_{ijkl}^{(n)}\varepsilon_{kl}^{(n)} - e_{kij}^{(n)}E_k^{(n)},\ \theta_3^{[n-1]} \le \theta_3 \le \theta_3^{[n]}, \quad (19)$$

$$D_i^{(n)} = e_{ikl}^{(n)}\varepsilon_{kl}^{(n)} + \in_{ik}^{(n)} E_k^{(n)},\ \theta_3^{[n-1]} \le \theta_3 \le \theta_3^{[n]}, \quad (20)$$

where $C_{ijkl}^{(n)}$, $e_{kij}^{(n)}$ and $\in_{ik}^{(n)}$ are the elastic, piezoelectric and dielectric constants of the *n*th layer.

Now, we accept the fifth and last assumption of the FG piezoelectric laminated shell formulation. Let us assume that the material constants are distributed through the thickness of the shell according to the following law

$$C_{ijkl}^{(n)} = \sum_{i_n} L^{(n)i_n} C_{ijkl}^{(n)i_n},\ e_{kij}^{(n)} = \sum_{i_n} L^{(n)i_n} e_{kij}^{(n)i_n},$$
$$\in_{ik}^{(n)} = \sum_{i_n} L^{(n)i_n} \in_{ik}^{(n)i_n} \quad (21)$$

that is extensively utilized in this paper, where $C_{ijkl}^{(n)i_n}$, $e_{kij}^{(n)i_n}$ and $\in_{ik}^{(n)i_n}$ are the values of elastic, piezoelectric and dielectric constants on SaS of the *n*th layer.

Finite Element Formulation

The variational equation (14) and (18) is the basis for developing the exact geometry (**EG**) four-node solid-shell element proposed in papers [7, 8]. The term EG reflects the fact that the parametrization of the middle surface is known and, therefore, coefficients of the first and second fundamental forms and Christoffel symbols are taken exactly at element nodes. In the EG shell element formulation, the displacement and electric field vectors of SaS of the *n*th layer are resolved in a surface frame $\mathbf{e}_i$. This in turn allows the implementation of the efficient *analytical integration* inside the EG solid-shell element.

The finite element formulation is based on the simple interpolation of the shell via curved EG four-node solid-shell elements

$$u_i^{(n)i_n} = \sum_r N_r u_{ir}^{(n)i_n},\ \varphi^{(n)i_n} = \sum_r N_r \varphi_r^{(n)i_n}, \quad (22)$$

where $\xi_\alpha = (\theta_\alpha - c_\alpha)/\ell_\alpha$ are the normalized curvilinear coordinates (see Fig. 2); $N_r(\xi_1, \xi_2)$ are the bilinear shape functions of the element; $u_{ir}^{(n)i_n} = u_i^{(n)i_n}(\widetilde{\mathrm{P}}_r)$ and $\varphi_r^{(n)i_n} = \varphi^{(n)i_n}(\widetilde{\mathrm{P}}_r)$ are the values of displacements and electric potentials of SaS at element nodes $\widetilde{\mathrm{P}}_r$ in (ξ_1, ξ_2)-space; the index *r* runs from 1 to 4 and denotes the number of nodes.

To implement the analytical integration throughout the EG shell element [7], we employ the assumed interpolation of strain and electric field components

$$\varepsilon_{ij}^{(n)i_n} = \sum_r N_r \varepsilon_{ijr}^{(n)i_n},\ \varepsilon_{ijr}^{(n)i_n} = \varepsilon_{ij}^{(n)i_n}(\widetilde{\mathrm{P}}_r), \quad (23)$$

$$E_i^{(n)i_n} = \sum_r N_r E_{ir}^{(n)i_n},\ E_{ir}^{(n)i_n} = E_i^{(n)i_n}(\widetilde{\mathrm{P}}_r). \quad (24)$$

Note that the main idea of such approach can be traced back to the ANS method (see, e.g. [9]). In contrast with the conventional ANS formulation, we treat the term "ANS method" in a broader sense. In our EG piezoelectric solid-shell element formulation, all strain and electric field components are assumed to vary bilinearly throughout the element. This implies that instead of the expected non-linear interpolation of strain and electric field components in accordance with equations (3), (4) and (10) the more suitable bilinear ANS interpolation is utilized. It is important that we advocate the use of the extended ANS method (23) and (24) to implement the efficient analytical integration inside the EG shell element.

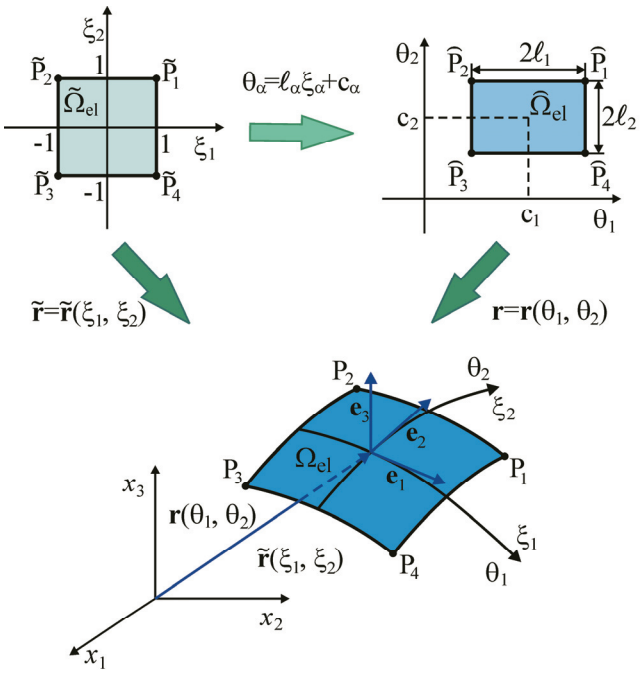

Fig. 2. Biunit square in (ξ_1, ξ_2)-space mapped into the EG shell element in (x_1, x_2, x_3)-space

Numerical Examples

1. First, we study a simply supported cylindrical shell with $L/R=4$ subjected to the sinusoidally distributed transverse load $\sigma_{33}^{[0]}=-p_0\sin\frac{\pi\theta_1}{L}\cos 4\theta_2$ at the bottom surface, where θ_1 and θ_2 are the longitudinal and circumferential coordinates of the middle surface; L and R are the length and radius of the shell. The shell is made of the unidirectional composite with the fibers oriented in the circumferential direction. The mechanical parameters are taken as $E_{\rm L}=25E_{\rm T}$, $G_{\rm LT}=0.5E_{\rm T}$, $G_{\rm TT}=0.2E_{\rm T}$, $E_{\rm T}=10^6$, $\nu_{\rm LT}=\nu_{\rm TT}=0.25$. Here, subscripts L and T refer to the fiber and transverse directions of the layer. To compare the derived results with the 3D exact solution [10], the following dimensionless variables are utilized:

$$\bar{u}_3=10E_{\rm L}h^3u_3(L/2,\,0,\,z)/R^4p_0,$$
$$\bar{\sigma}_{22}=10h^2\sigma_{22}(L/2,\,0,\,z)/R^2p_0,$$
$$\bar{\sigma}_{13}=100h\sigma_{13}(0,\,0,\,z)/Rp_0,$$
$$\bar{\sigma}_{23}=10h\sigma_{23}(L/2,\,\pi/8,\,z)/Rp_0,\quad z=\theta_3/h.$$

Due to symmetry of the problem, only one sixteenth of the shell is discretized using the 32×128 mesh of EG four-node solid-shell elements. The data listed in Table 1 demonstrate the high potential of the developed SaS finite element formulation, which provides three right digits for basic variables at crucial points utilizing seven SaS inside the moderately thick and thin shells.

2. Consider next a symmetric piezoelectric three-layer cylindrical shell with equal ply thicknesses subjected to mechanical loading acting on the top surface

$$\sigma_{13}^{[0]}=\sigma_{23}^{[0]}=\sigma_{33}^{[0]}=\varphi^{[0]}=\sigma_{13}^{[3]}=\sigma_{23}^{[3]}=\varphi^{[3]}=0,$$
$$\sigma_{33}^{[3]}=p_0\sin\frac{\pi\theta_1}{L}\cos\theta_2$$

or electric loading acting on the same surface

$$\sigma_{13}^{[0]}=\sigma_{23}^{[0]}=\sigma_{33}^{[0]}=D_3^{[0]}=\sigma_{13}^{[3]}=\sigma_{23}^{[3]}=\sigma_{33}^{[3]}=0,$$
$$D_3^{[3]}=q_0\sin\frac{\pi\theta_1}{L}\cos\theta_2,$$

where $p_0=-1$ Pa and $q_0=1$ C/m^2. The bottom and top layers are composed of the FG piezoelectric material, whereas the central layer is made of the homogeneous piezoelectric material. It is assumed that the FG material properties are distributed in the thickness direction according to the exponential law [1]

$$C_{ijkl}^{(1)}=C_{ijkl}^{(2)}e^{\mu_1(z)},\ e_{ikl}^{(1)}=e_{ikl}^{(2)}e^{\mu_1(z)},$$
$$\in_{ik}^{(1)}=\in_{ik}^{(2)}e^{\mu_1(z)},\quad -1/2\le z\le -1/6,$$
$$C_{ijkl}^{(3)}=C_{ijkl}^{(2)}e^{\mu_3(z)},\ e_{ikl}^{(3)}=e_{ikl}^{(2)}e^{\mu_3(z)},$$
$$\in_{ik}^{(3)}=\in_{ik}^{(2)}e^{\mu_3(z)},\quad 1/6\le z\le 1/2,$$
$$\mu_1(z)=-\alpha(6z+1)/2,$$
$$\mu_3(z)=\alpha(6z-1)/2,$$
$$z=\theta_3/h,$$

where α is the material gradient index; $C_{ijkl}^{(2)}$, $e_{ikl}^{(2)}$ and $\in_{ik}^{(2)}$ are the elastic, piezoelectric and dielectric constants of the central layer, which are considered to be the same as those of the PZT-4, whose material properties are given in [1, 4].

The geometric parameters of the shell are taken to be $L=4$ m and $R=1$ m. To compare the results derived with the analytical solution [1], we introduce

Table 1

Results for the composite cylindrical shell using seven SaS and 32×128 mesh

R/h	EG solid-shell element formulation				Varadan and Bhaskar [10]			
	$\bar{u}_3(0)$	$\bar{\sigma}_{22}(0.5)$	$\bar{\sigma}_{13}(0)$	$\bar{\sigma}_{23}(0)$	$\bar{u}_3(0)$	$\bar{\sigma}_{22}(0.5)$	$\bar{\sigma}_{13}(0)$	$\bar{\sigma}_{23}(0)$
4	2.782	4.854	0.9863	–2.970	2.783	4.859	0.987	–2.990
10	0.9188	4.048	0.5199	–3.665	0.9189	4.051	0.520	–3.669
100	0.5169	3.840	0.3927	–3.856	0.5170	3.843	0.393	–3.859

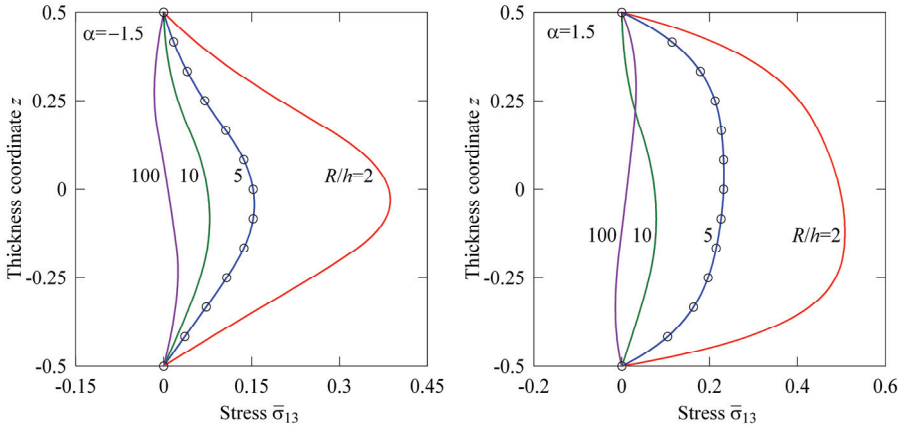

Fig. 3. Through-thickness distribution of transverse shear stresses of the FG three-layer cylindrical shell under mechanical loading:
EG finite element formulation (—) and analytical solution [1] (○)

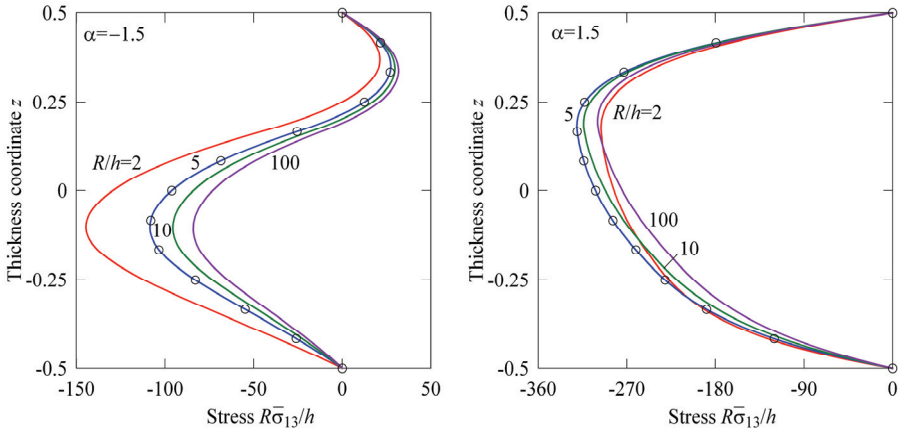

Fig. 4. Through-thickness distribution of transverse shear stresses of the FG three-layer cylindrical shell under electric loading:
EG finite element formulation (—) and analytical solution [1] (○)

dimensionless variables $\bar{\sigma}_{13} = \sigma_{13}(0, 0, z)/p_0$ in the case of mechanical loading and $\bar{\sigma}_{13} = 10^{-6} \times \times \sigma_{13}(0, 0, z) q^*/p^* q_0$ in the case of electric loading, where $p^* = 1$ N/m^2, $q^* = 1$ C/m^2 and $z = \theta_3/h$.

Figures 3 and 4 display the distribution of transverse shear stresses in the thickness direction for different values of the slenderness ratio *R/h* and the material gradient index α employing nine SaS for each layer and the 64×64 uniform mesh of EG four-node solid-shell elements. These results demonstrate again the high potential of the proposed SaS solid-shell element formulation. This is due to the fact that boundary conditions on the bottom and top surfaces and continuity conditions at interfaces for transverse shear stresses are satisfied exactly.

Conclusions

The SaS formulation for the 3D analysis of FG piezoelectric laminated shells has been developed. This formulation is based on choosing the SaS located at Chebyshev polynomial nodes throughout the layers. Such choice permits one to minimize uniformly the error due to Lagrange interpolation. The SaS formulation for piezoelectric laminated shells is based on 3D constitutive equations and gives the possibility to obtain 3D solutions for FG piezoelectric shells with a prescribed accuracy, which asymptotically approach the exact solutions of piezoelectricity as the number of SaS goes to infinity.

References

1. Wu, C. P., & Tsai, T. C. (2012). Exact solutions of functionally graded piezoelectric material sandwich cylinders by a modified Pagano method. Applied Mathematical Modelling, 36, 1910-1930.

2. Kulikov, G. M., & Plotnikova, S. V. (2013). A new approach to three-dimensional exact solutions for functionally graded piezoelectric laminated plates. Composite Structures, 106, 33-46.

3. Kulikov, G. M., & Plotnikova, S. V. (2013). A sampling surfaces method and its application to three-dimensional exact solutions for piezoelectric laminated shells. International Journal of Solids and Structures, 50, 1930-1943.

4. Kulikov, G. M., & Plotnikova, S. V. (2014). Exact electroelastic analysis of functionally graded piezoelectric shells. International Journal of Solids and Structures, 51, 13-25.

5. Burden, R. L., & Faires, J. D. (2010). Numerical analysis (9th ed.). Boston: Brooks/Cole, Cengage Learning.

6. Kulikov, G. M., & Plotnikova, S. V. (2013). Advanced formulation for laminated composite shells: 3D stress analysis and rigid-body motions. Composite Structures, 95, 236-246.

7. Kulikov, G. M., & Plotnikova, S. V. (2007). Non-linear geometrically exact assumed stress-strain four-node solid-shell element with high coarse-mesh accuracy. Finite Elements in Analysis and Design, 43, 425-443.

8. Kulikov, G. M., & Plotnikova, S. V. (2011). Non-linear exact geometry 12-node solid-shell element with three translational degrees of freedom per node. International Journal for Numerical Methods in Engineering, 88, 1363-1389.

9. Hughes, T. J. R. (1987). Finite element method: linear static and dynamic finite element analysis. New Jersey: Prentice Hall.

10. Varadan, T. K., & Bhaskar, K. (1991). Bending of laminated orthotropic cylindrical shells – an elasticity approach. Composite Structures, 17, 141-156.